Canadian Mineralogist
Vol. 26, pp. 841-858 (1988)

GEOCHEMICAL ASPECTS OF HYDROTHERMAL SEDIMENTS IN THE EASTERN PACIFIC OCEAN: AN UPDATE

TIMOTHY J. BARRETT
Mineral Exploration Research Institute, Department of Geological Sciences, McGill University,
3450 University Street, Montreal, Quebec H3A 2A7

IAN JARVIS
School of Geological Sciences, Kingston Polytechnic, Kingston-on-Thames, Surrey, Great Britain KT1 2EE

FRED J. LONGSTAFFE
Department of Geology, University of Western Ontario, London, Ontario N6A 5B7

RON FARQUHAR
Department of Physics, University of Toronto, Toronto, Ontario M5S 1A7

ABSTRACT

Metalliferous sediments in the eastern central Pacific are represented mainly by a Fe–Mn-rich oxyhydroxide component, both in surficial sediments up to 2000 km from the East Pacific Rise and in sediments overlying basaltic basement as old as Paleocene age. On a carbonate-free basis, these and other (non-nodule) metalliferous sediments in the eastern Pacific typically contain ≈25–35% Fe, 5–10% Mn, 1000–2000 ppm Cu, 500–1000 ppm Zn and Ni, and <250 ppm Co and Pb. Fe/Mn ratios for the metalliferous component generally increase with distance from the paleo-axis, whereas Fe/Al ratios and the mass accumulation rates of Fe, Mn and base metals decrease. These trends reflect decreasing fallout of particulate matter from dilute hydrothermal plumes. Much of the Pb in the sediments is of basaltic–hydrothermal origin as far as 250 km from the axis, with mixed basaltic–seawater Pb beyond this, whereas the rare earth elements (*REE*) and Sr are of seawater derivation. In some areas of the eastern Pacific, Fe-rich smectite is the main hydrothermal phase, and probably is a byproduct of early diagenetic reaction between biogenic silica and hydrothermal Fe–Mn-rich oxyhydroxides. In the Galapagos mounds field, nontronite is the main hydrothermal component. Here, nontronite has formed because a high rate of biogenic sedimentation allowed solutions upwelling from the basement to penetrate and react with the sediment cover. Oxygen isotope data for nontronite suggest that it generally formed at <30°C. Pb in the nontronite is commonly more radiogenic than either basaltic or seawater sources, for which there is no clear explanation. The *REE* in nontronite are interpreted to have been inherited mainly from seawater, although Ce anomalies are less negative than that of seawater. Granular nontronite has lower *REE* concentrations than nontronite in finer grained transitional zones, suggesting *REE* expulsion as granules formed. Within the axial valley of the Southern Explorer Ridge in the northeast Pacific, thin oxidized sediments overlie massive sulfide mounds. *In situ* oxidation of sulfides/sulfates produces an initial alteration gossan dominated by Fe oxyhydroxide phases. With continued exposure of the mound surface, it is suggested that Fe/Mn ratios decrease, sulfates break down with net loss of Sr, and the proportion of volcaniclastic material increases. Studies by other workers on ridge-proximal hydrothermal smoke and sediments in the eastern Pacific indicate that Fe–Mn oxyhydroxides become an important component of the hydrothermal plume soon after discharge, either as direct precipitates or through oxidation of sulfide particles.

Keywords: hydrothermal sediments, Fe–Mn oxyhydroxides, nontronite, isotopes, *REE*, geochemistry, genesis, eastern Pacific Ocean.

SOMMAIRE

Les sédiments métallifères de la partie est-centrale du Pacifique contient surtout une composante à oxyhydroxyde riche en Fe–Mn, aussi bien dans les sédiments de surface, jusqu'a 2000 km de la crête Est-Pacifique, que dans les sédiments recouvrant le socle basaltique, qui atteint un âge paléocène. Reconstitués sans carbonates, ces sédiments du Pacifique oriental, et les autres sans nodules, contiennent de 25 à 35% Fe, de 5 à 10% Mn, 1000–2000 ppm Cu, 500–1000 ppm Zn et Ni, et moins de 250 ppm Co et Pb. Le rapport Fe/Mn du composant métallifère diminue généralement avec la distance d'une paléo-ride, tandis que le rapport Fe/Al et le taux d'accumulation de Fe, de Mn et des métaux de base diminuent. Ces tendances témoignent d'une diminution dans la quantité de particules sulfurées des panaches hydrothermaux dilués. Une grande proportion du Pb des sédiments a une origine basaltique - hydrothermale, même à 250 km de l'axe; la source est mixte (basalte - eau de mer) à des distances plus grandes. Les terres rares et le Sr sont dérivés de l'eau de mer. Dans certaines régions, une smectite riche en fer constitue le minéral métallifère le plus important; elle serait un sous-produit d'une réaction diagénétique précoce entre silice biogénique et oxyhydroxydes riches en Fe–Mn d'origine hydrothermale. Les sédiments des amoncèlements de Galapagos contiennent surtout des intercalations lenticulaires de nontronite à grains grossiers et de boues riches en carbonates, séparées par des zones transitionnelles riches en nontronite à grains fins. Cette séquence est recouverte de croûtes à oxydes de Mn. Cette nontronite se serait formée suite au taux élevé de sédimentation biogénique, ce qui a permis aux solutions dérivées du socle de pénétrer et de réagir avec la couverture sédimentaire. Les données sur les isotopes d'oxygène font penser que la nontronite s'est formée à moins de 30°C. D'après les signatures isotopiques, le Pb provient de deux sources: un mélange du Pb de l'eau de mer et de basaltes, et, de façon plus équivoque, du Pb d'une cendre volcanique radiogénique. Les teneurs en terres rares de la nontronite seraient dues aux contributions des boues carbonatées dissoutes et d'une fraction résiduelle à caractère clastique-basaltique moins importante. La nontronite à grains grossiers est plus faible en terres rares que la nontronite des zones de transition, ce qui fait penser qu'il y a eu expulsion des terres rares lors de la formation des granules. Au sein de la vallée axiale de la crête dite de Southern Explorer, une mince couche de sédiments oxydés recouvre les amoncèlements de sulfures massifs. Les données géochimiques témoignent d'une oxydation *in situ* des sulfures et des sulfates, produisant d'abord un gossan où prédominent les oxyhydroxydes de fer. Dans la surface exposée de l'amoncèlement, la valeur du rapport Fe/Mn diminue, les sulfates sont détruits, avec perte nette du Sr, et le degré d'altération du matériau volcaniclastique augmente avec le temps. Les résultats d'autres études des panaches hydrothermaux près des rides et des sédiments associés dans le bassin Pacifique oriental montrent que les oxyhydroxydes de Fe–Mn deviennent importants dans le panache tôt après une décharge, suite à une précipitation directe ou par oxydation des particules de sulfures.

(Traduit par la Rédaction)

Mots-clés: sédiments hydrothermaux, oxyhydroxydes de Fe–Mn, nontronite, isotopes, terres rares, géochimie, genèse, bassin Pacifique oriental.

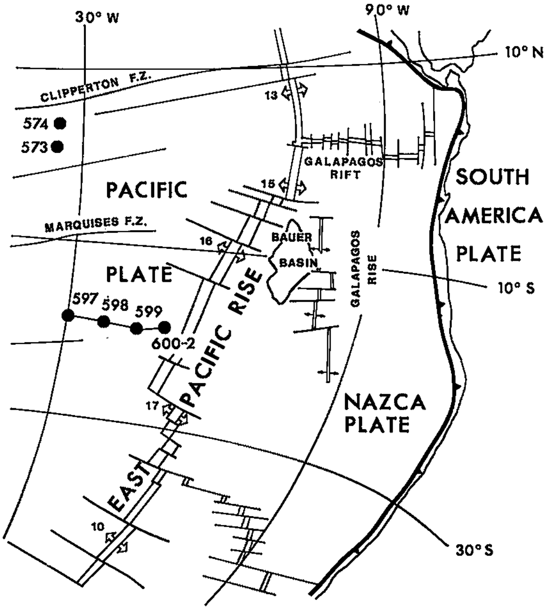

FIG. 1. Index map of the eastern Pacific showing the location of Leg 92 Sites 597 to 602 (the EPR transect), together with DSDP Sites 573 and 574 (Leg 85) on the Pacific Plate. Numbers and arrows on spreading axes refer to total rate (cm/yr) and direction of spreading (Circum-Pacific Council for Energy and Mineral Resources Map, 1981).

INTRODUCTION

Metalliferous sediments have been recovered from localities ranging from a few km to a few thousand km from the main axes of spreading in the eastern Pacific. Studies of the mineralogy, geochemistry, and origin of recent metalliferous sediments (Fig. 1) have concentrated on the East Pacific Rise (Boström & Peterson 1966, Bender *et al.* 1971, Sayles & Bischoff 1973, Piper 1973, Dymond & Veeh 1975, Heath & Dymond 1977, 1981, Marchig & Gundlach 1982, Bäcker *et al.* 1985, Marchig *et al.* 1986), the Bauer Deep (Sayles *et al.* 1975, Dymond 1981, McMurtry *et al.* 1981, Lyle 1981, Field *et al.* 1981), and the Galapagos hydrothermal mounds field (Corliss *et al.* 1978, Hékinian *et al.* 1978, Williams *et al.* 1979, Barrett & Friedrichsen 1982, Varnavas *et al.* 1983, Honnorez *et al.* 1981, Moorby 1983, McMurtry *et al.* 1983). Studies of East Pacific Rise (EPR) sediments have concluded that an initial metalliferous component, consisting of ferromanganiferous oxyhydroxide precipitates enriched in trace elements, was derived from hydrothermal activity at the ridge axis. Oceanographic and chemical evidence indicates that the precipitates are dispersed by dilute hydrothermal plumes in the lower water column for lateral distances up to 10^3 km (Lupton & Craig 1981, Klinkhammer & Hudson 1986) before settling out into pelagic sediments (Heath & Dymond 1981, Edmond *et al.* 1982, Baker *et al.* 1985). An important exception to this mode of formation are the nontronite-rich deposits at the Galapagos hydrothermal mounds, located about 20–30 km from the Galapagos spreading axis (Natland *et al.* 1979, Honnorez *et al.* 1981). These deposits form mainly within the sediment column in response to low-temperature reactions between hydrothermal solutions and biogenic sediment. The present paper, which is mainly a review, deals firstly with oxyhydroxide-rich metalliferous sediments in the eastern central Pacific, then with the nontronite-rich deposits in the Galapagos hydrothermal mounds field, and finally with a preliminary study of thin oxidized sediments that overlie massive sulfides on the Southern Explorer Ridge in the northeast Pacific. Further data are presented in the second and third parts of the paper.

METHODS

Oxygen isotopes

Splits of sample powders were analyzed at the University of Alberta. Oxygen was extracted using the bromine pentafluoride procedure (Clayton & Mayeda 1963). Oxygen isotopic compositions are reported using normal δ-notation relative to Standard Mean Ocean Water. Routine reproducibility of $\delta^{18}O$ values is typically 0.15‰. Temperatures of formation of nontronite were estimated from the oxygen isotopic compositions by applying the formula of Yeh & Savin (1977) for normal smectite. No corrections were made for the higher Fe/Al ratios of the nontronite, as no suitable data are as yet available to permit correlation between Fe content (or Mg or Al content) and $\delta^{18}O$ values of authigenic marine smectites. In the temperature calculations, it is assumed that the nontronite formed from normal seawater with a $\delta^{18}O$ value of zero. The Ca values in mound pore waters (Maris *et al.* 1984), together with the empirical relationship between Ca concentration and $\delta^{18}O$ values of DSDP sediment pore waters (Lawrence & Gieskes 1981) suggest that solutions in the mounds are not depleted by more than 1‰, which would yield temperature estimates ≈5°C too high.

Lead isotopes

About 100 mg of sample powder were used for analysis of Leg 70 samples. All samples were washed in purified water using ultrasonic agitation. One sample (507D-6-3) also was washed in acetic acid to remove biogenic carbonate. Samples were decomposed with HF and HNO_3 in teflon capsules. Pb was separated using an anion exchange column with 1*N* HBr. Pb was further purified on a second anion exchange column with 1*N* HCl. The total procedural blank was about 0.5 ng, which does not significantly affect the isotopic composition of the samples. Pb isotopic compositions were determined at the University of Toronto using the silica gel–H_3PO_4 method with a custom-built mass spectrometer (30 cm radius, 90° sector). All data were corrected for a mass discrimination factor of 0.140 ± 0.025% per a.m.u. as determined by replicate analysis of isotopic standard SRM-981. Analytical methods for the Leg 92 sediments are given in Barrett *et al.* (1987).

Rare-earth elements

Samples weighing ≈0.5 g were dissolved using aqua regia, then HF–$HClO_4$ acid treatments. A sequential cation-exchange procedure was then used to isolate the *REE* (Jarvis & Jarvis 1985). La, Ce, Pr, Nd, Sm, Eu, Gd, Dy, Ho, Er, Yb, Lu, and Y were determined sequentially using an ARL 3510 inductively coupled plasma–atomic emission spectrometer (ICP–AES) in the Department of Geology, City of London Polytechnic. Analytical precision as determined by replicate analyses is better than ± 3% for all *REE* exceeding 0.2 ppm. By reference to international standards, absolute accuracy is judged to be better than ±10% of the quoted values (Jarvis & Jarvis 1988). In this paper, normalized *REE* concentrations are reported relative to USGS standard SCo-1 (Cody shale) (Table 1). The pattern for this standard is very similar to that of other 'average' post-Archean shales (Haskin & Haskin 1966).

TABLE 1. COMPOSITION OF NONTRONITIC SEDIMENTS FROM THE GALAPAGOS HYDROTHERMAL MOUNDS, DSDP LEG 70

Sample	SiO_2	TiO_2	Al_2O_3	Fe_2O_3	MnO	MgO	CaO	Na_2O	K_2O	P_2O_5	Ba ppm	Cr ppm	Zn ppm	LOI	Total	Fe_2O_3/ SiO_2
506-6-2: 24-25	53.26	0.03	0.74	28.95	0.04	4.37	0.27	2.24	3.44	0.03	439	14	32	6.88	100.3	.543
506-6-2: 65-67	52.40	0.01	0.19	30.56	0.05	4.48	0.21	1.44	4.56	0.04	211	13	26	5.90	99.86	.583
507D-6-2: 130-132	53.07	0.01	0.01	30.14	0.05	4.74	0.15	1.94	3.76	0.02	49	13	35	6.23	100.1	.568
509B-1-2: 124-125	49.44	0.02	0.54	31.25	2.23	3.33	0.40	2.50	1.84	0.04	183	18	nd	8.16	99.77	
509B-3-1: 142-144	52.55	0.01	0.03	31.37	0.08	3.61	0.29	2.35	2.77	0.02	37	13	18	6.77	99.86	.597

Values in % unless otherwise noted. Total iron expressed as Fe_2O_3.

V and Ni <10 ppm in all samples.

Nontronite type given in Table 2 (509B-1-2: 124-125 contains Mn oxides).

Leach methods

The sediment analyses in the first and last parts of the paper were performed on the <200 mesh fraction of the sediments, following a series of leach treatments (similar to those of Chester & Hughes 1967, as described in Barrett *et al.* 1986). The first acid leach (L-1) is intended to remove biogenic carbonate. The second leach (L-2) removes amorphous and poorly crystallized Fe oxyhydroxides and manganiferous phases, whereas the third (L-3) removes well-crystallized Fe oxyhydroxides. Together, L-2 and L-3 mainly remove the hydrothermal metalliferous component, although authigenic phases such as Fe-rich smectite and basaltic alteration products can also be partly attacked.

OPEN-OCEAN METALLIFEROUS SEDIMENTS

Deep Sea Drilling Project (DSDP) Leg 92 recently drilled at four sites, located ≈350 to 1150 km from the spreading axis of the EPR, along an east-west transect at 19°S (Fig. 1). This transect is ideal for the study of the relation of metalliferous sedimentation to seafloor spreading because this segment of the EPR has a high spreading rate and a well-known tectonic history during the Neogene (Rea & Leinen 1986). In addition, the existence of a major hydrothermal plume extending at least 1400 km west of the EPR near 19°S has been documented (Lupton & Craig 1981, Klinkhammer & Hudson 1986). Finally, clastic sedimentation to the west of the EPR is almost negligible, so that the sediments are mainly mixtures of hydrothermal and biogenic carbonate components.

Leg 92 sediments are calcareous nannofossil oozes with variable admixtures (commonly 20 to 40%) of a darker, fine-grained metalliferous component of Fe oxides and hydroxides, red-brown to yellow-brown semi-opaque oxides, and poorly crystalline smectitic clays (Leinen *et al.* 1986). The dominant crystalline phases are moderately to well-crystallized goethite, with minor proportions of apatite and traces of quartz in some samples. Leach treatments suggest that X-ray amorphous Fe-Mn oxyhydroxides constitute some 30-50% of the metalliferous component, and that some poorly crystalline goethite is also present (Barrett *et al.* 1987).

Major and trace elements

On a carbonate-free, salt-free basis, the metalliferous component of Leg 92 sediments (Barrett *et al.* 1987) is characterized by: (i) very high concentrations of Fe and Mn, typically 25–39% and 5–14%, respectively; (ii) Al and Ca contents generally less than 2% and 5%, respectively; (iii) high Cu (1000–2000 ppm), and high Zn and Ni (500–1000 ppm) values; and (iv) Co and Pb generally <250 ppm. Similar results were obtained by Lyle (1986) for the Leg 92 carbonate-free fraction. Concentrations of Fe, Mn and base metals are comparable to, but somewhat higher than at other Pacific DSDP sites which encountered metalliferous sediments (Tracey *et al.* 1971, von der Borch *et al.* 1971, Hays *et al.* 1972, van Andel *et al.* 1973, Dymond *et al.* 1973, Cronan 1973, 1976, Yeats *et al.* 1976, Leinen 1981, Mayer *et al.* 1985).

The Fe concentrations in Leg 92 sediments approximate those in sediments occurring within ≈40 km of the EPR at 18.5°S (Bäcker *et al.* 1985), whereas Mn concentrations and Fe/Mn ratios generally become greater with increasing distance from the EPR (Lyle 1986). From base to top of a given drill site along the Leg 92 transect (*i.e.*, as individual sites moved away from the axis), Fe/Al ratios also decrease significantly (Lyle *et al.* 1986), reflecting decreasing hydrothermal influence. The Fe/Mn ratio increases apparently as a result of settling out of a significant fraction of the Mn in the hydrothermal plume (dissolved or particulate) within ≈200–300 km of the axis. The Fe/Mn ratio near the basaltic basement in each hole is ≤3, similar to the value of 3 to 4 for surficial sediments up to 40 km from the EPR axis (Bäcker *et al.* 1985), and for end-member 350°C solutions at 21°N (Von Damn *et al.* 1985). Trace-element contents of Leg 92 sediments compare closely with those of surficial sediments on the EPR crest (Boström *et al.* 1969, Bender *et al.* 1971, Bäcker *et al.* 1985), and to near-basal 11–15 Ma sediments cored at Site 319, located in the Bauer Deep 1100 km east of the EPR (Dymond *et al.* 1976).

The mass accumulation rates of Fe, Mn, Cu and Pb in Leg 92 sediments are greatest near the basement at each site, with a general decrease towards the top of the each hole (Lyle *et al.* 1986, Barrett *et al.* 1987). Similar trends and absolute values have been reported for the lower part of the section at Site 319 in the Bauer Deep (Dymond *et al.* 1976). Surface sediments west of the EPR also show a decrease in the mass accumulation rate of the hydrothermal component with distance from the ridge (Dymond 1981). In general, there is a logarithmic decrease in the hydrothermal input to the bulk sediment with migration of the crust from the axis (Rea & Leinen 1986). Site 597 (Fig. 1) also shows a second, distinct peak in the accumulation rates of Fe and Mn at ≈17–18 Ma ago, which probably reflects a resurgence in hydrothermal supply related to a ridge jump from the ancient Mendoza Rise to the present position of the EPR (Lyle *et al.* 1986).

Mass accumulation rates for Leg 92 sediments deposited within ≈250 km of the paleorise have Fe, Mn, Cu and Pb values in the respective ranges of 40–96, 10–35, 0.10–0.44, and 0.02–0.07 mg/cm^2/1000 yr (Barrett *et al.* 1987; see also Lyle *et al.* 1986). On the large abyssal plains of the ocean floor, the accumulation rates of metals in pelagic red clays are vastly lower: <0.003 mg/cm^2/1000 yr for Fe and Mn, and <10^{-4} mg/cm^2/1000 yr for Cu, Ni, Zn and Co (Thomson *et al.* 1984). The differences between mass accumulation rates of metals in Leg 92 basal sediments and "background" values from the abyssal plain areas should approximate hydrothermal fluxes in the near-rise environment of the EPR.

The metalliferous component of sediments in some parts of the eastern Pacific ocean is represented by an Fe smectite rather than by Fe–Mn oxyhydroxide phases. Fe smectite dominates surface sediments in the Bauer Deep (Sayles *et al.* 1975, Heath & Dymond 1981, Cole 1985) and in other areas of slow sediment accumulation in the Pacific Ocean (Aoki *et al.* 1974, Hein *et al.* 1979). At DSDP Site 319 in the Bauer Deep, Fe smectite is an important phase in the upper ≈11 Ma of the sediment column. At Sites 573 and 574 (Fig. 1), two metalliferous phases have been identified in near-basal Eocene–Oligocene sediments, one rich in Fe smectite, the other in Fe–Mn oxyhydroxide phases (Jarvis 1985). Fe smectite evidently becomes an important phase in the metalliferous component if the supply of biogenic silica to the seafloor is sufficient. During early diagenesis, primary oxyhydroxides of hydrothermal derivation react with silica released from dissolving biogenic material to form the Fe smectites (Heath & Dymond 1977, Lyle 1981).

Pb isotopes

In open-ocean sediments little is known about the proportion of metals which is actually derived from the basaltic crust, as opposed to the proportion extracted from seawater by the hydrothermal ferromanganiferous precipitates. Pb isotopes provide one of the best tools for unambiguously determining the relative contributions of these sources. Pb isotope results for Leg 92 sediments (Fig. 2) form approximately linear arrays in the two isotopic plots (excluding two anomalous samples; Barrett *et al.*

1987). The less radiogenic portions of the arrays have Pb isotope compositions typical of oceanic crust in the eastern–northeastern Pacific. The more radiogenic portions approach the field of manganese nodules, which reflects the Pb isotope composition of seawater. Intervening data on the plots are most readily interpreted in terms of simple linear mixing of basalt- and seawater-derived Pb. Leg 92 sediments deposited up to 3.5 Ma after formation of underlying basement contain 80–100% basaltic-hydrothermal Pb, indicating such Pb can be dispersed up to 250 km from the rise (using spreading rates from Rea & Leinen 1986). In the eastern Pacific, sediments with a large component of basaltic Pb occur on the EPR (Bender *et al.* 1971), in the Bauer Deep (Dasch *et al.* 1971, Unruh & Tatsumoto 1976, Dymond 1981), and in DSDP sediments overlying basaltic basement (Dymond *et al.* 1973).

The average of the four least radiogenic samples in the Leg 92 sample set (small ovals in Fig. 2) lies near the middle of Sun's (1980) field for mid-ocean ridge basalts, and close to the Pb isotope composition of discharging hydrothermal solutions in the eastern Pacific (Chen 1987). The end-member value also is very close to the average Pb isotope composition of basaltic oceanic crust in the eastern Pacific (Church & Tatsumoto 1975, Zindler *et al.* 1982), and to massive sulfides forming from 350°C solutions at the EPR axis at 21°N (Vidal & Clauer 1981, Brevart *et al.* 1981). Although hydrothermal solutions must lose some of their basaltic Pb to directly precipitated sulfides (at and/or below the seawater interface), sufficient Pb evidently is incorporated into seawater precipitates to produce metalliferous sediments whose Pb isotope composition closely matches the average of the underlying basaltic crust.

Sr isotopes

The evolution of the Sr isotopic composition of seawater with time has been documented by Veizer & Compston (1974) and refined by Burke *et al.* (1982) and DePaulo & Ingram (1985). These studies have used biogenic carbonate to monitor the variations, which are largely controlled by the average Sr isotopic composition of continental runoff into the oceans (the present $^{87}Sr/^{86}Sr$ ratio of seawater is ≈ 0.7091). Because oceanic crust has a distinctively lower $^{87}Sr/^{86}Sr$ ratio of ≈ 0.7027, it should be possible to detect a basaltic–hydrothermal input into metalliferous sediments. Barrett *et al.* (1986) found that Sr isotopic ratios of the metalliferous component in Leg 92 sediments up to ≈ 25 Ma old became lower with increasing age, and generally were close to the seawater curve. Although the lowered values could reflect some basaltic–hydrothermal contribution, the simplest explanation is that seawater Sr either was absorbed into the metalliferous component during sedimentation, or was released from biogenic carbonate during burial and dissolution and was incorporated into the metalliferous component. Seawater Sr dominates the metalliferous component, even though basalts contain two orders of magni-

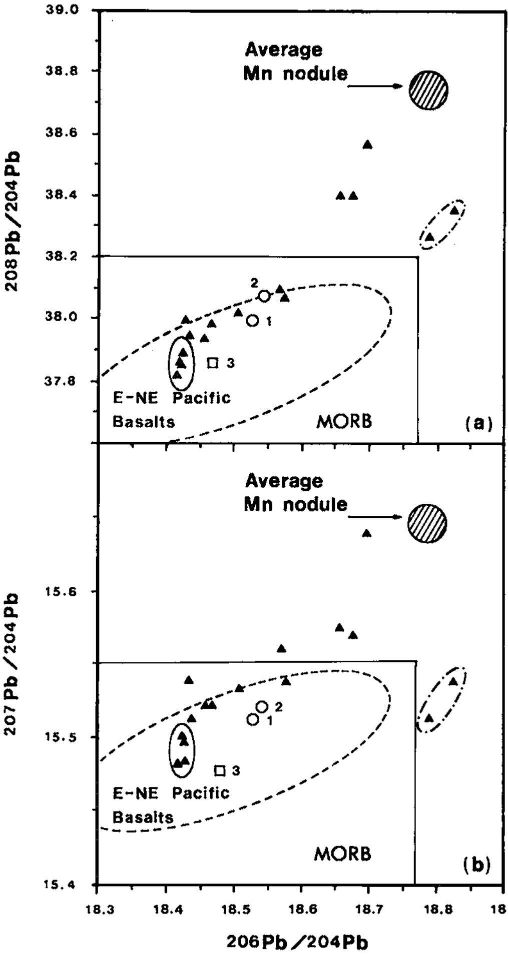

FIG. 2. Pb isotope data for metalliferous sediments from Sites 597 to 601, DSDP Leg 92 (triangles). Data are for carbonate-free samples (Barrett *et al.* 1987). Two anomalous samples are enclosed by dot-dash line. The oceanic Mn nodule average is from the data of Reynolds & Dasch (1971) and Stacey & Kramers (1975); average pelagic sediment (Stacey & Kramers 1975) also plots very close to this value. The field of Pacific-ridge basalts (dashed lines) is from Church & Tatsumoto (1975) and Zindler *et al.* (1982); the MORB field (boxes) is from Sun (1980). Also shown are the Pb isotopic compositions of: (1): surficial metalliferous sediments from the EPR (O'Nions *et al.* 1978); (2): basal metalliferous sediments ≈ 15 Ma old from the Bauer Deep (Unruh & Tatsumoto 1976); and (3): average massive sulfides from 21°N EPR (Brevart *et al.* 1981, Vidal & Clauer 1981).

tude more Sr than Pb (Church & Tatsumoto 1975, Hart 1976), because seawater contains six orders of magnitude more Sr than Pb (Veizer & Compston 1974, C.C. Patterson, in Tatsumoto 1978). In addition, basaltic Pb should be less soluble than Sr in reducing fluids and should follow Fe as a sulfide precipitate in smoke formed at hydrothermal vents, whereas basaltic Sr will be diluted by ambient seawater (Chen *et al.* 1986).

Rare-earth elements

Fe–Mn oxyhydroxide-rich sediments ≈20 to 40 km west of the black-smoker areas of the EPR at 18.5°S have *REE* patterns closely similar to those of normal seawater (Marchig *et al.* 1986), as do surficial sediments from the crest of the EPR, ≈150–230 km from the axis (Piper & Graef 1974). Shale-normalized *REE* patterns for the carbonate-free fraction of Leg 92 samples less than about 8 Ma old are shown in Figure 3 (data in Barrett & Jarvis 1988). Samples older than about 10 Ma (not shown) are somewhat enriched in the middle to light rare earths (*MREE* to *LREE*) relative to the heavy rare earths (*HREE*). Within each age group, the characteristics of the *REE* patterns are near-uniform, even though total *REE* concentrations vary up to a factor of six (Barrett & Jarvis 1988). All patterns have strongly negative Ce anomalies. These results are generally similar to those of Ruhlin & Owen (1986), who carried out a detailed *REE* study of sediments from Site 598.

A direct hydrothermal source for the *REE* in these

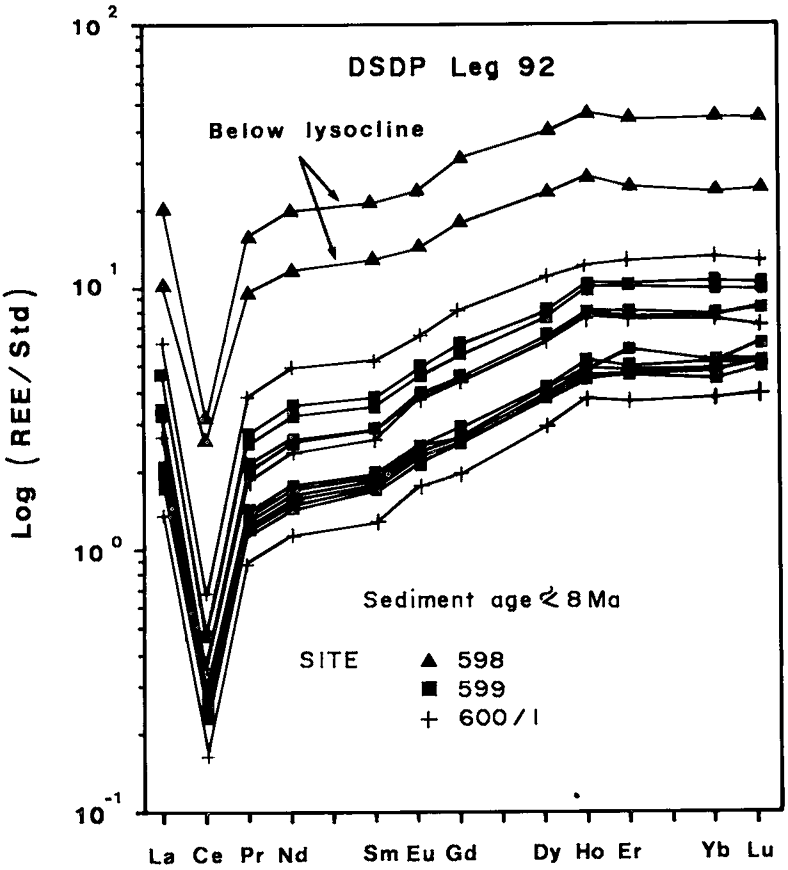

FIG. 3. *REE* patterns for Leg 92 metalliferous sediments younger than ≈8 Ma (Barrett & Jarvis 1988). Note close similarity of all patterns except for the two *REE*-enriched near-surface sediments deposited below the lysocline (core 598-1). *REE* patterns for metalliferous samples older than ≈10 Ma are also internally consistent, but differ in having a greater enrichment in the middle to light *REE* relative to the *HREE*. Values normalized to USGS standard shale SCo-1 (Jarvis & Jarvis 1985).

metalliferous sediments is unlikely. High-temperature (350°C) solutions discharging at the EPR are characterized by large positive Eu anomalies and depletions in the *HREE* relative to the *LREE*, probably the result of reactions between normal seawater and basaltic crust in the deep subsurface (Michard *et al.* 1983). The seawater-like pattern of EPR sediments apparently results from the rapid adsorption of seawater *REE* onto hydrothermally derived Fe-Mn oxyhydroxide colloidal particles, either in the water column or after the particles have settled onto the seafloor. The enrichment in Leg 92 sediments of the middle to light *REE* relative to deep plume seawater at the same latitude supports the inference (Klinkhammer *et al.* 1983) that hydrothermal precipitates preferentially remove the lighter *REE* from seawater. Removal of the lighter *REE* probably reflects the longer residence time of *HREE* in the deep ocean (Elderfield & Greaves 1982). The longer residence time may result from the greater stability of (dissolved) *HREE* complexes relative to *LREE* complexes in seawater (Turner *et al.* 1981).

The mass accumulation rate of Σ*REE* shows a moderate correlation with that of combined Fe + Mn, which decreases with distance above basement (Barrett & Jarvis 1988). Similar relations (using Fe rather than Fe + Mn) were documented by Ruhlin & Owen (1986) at Site 598, and were attributed to limited scavenging of *REE* (producing low Σ*REE*) due to rapid accumulation of sediment (producing high accumulation rates) near the paleo-axis. With recession of a site from the hydrothermal source, precipitates would have travelled farther and scavenged more *REE* before settling from the water column (accumulation rates still decrease upward at each site).

Leg 92 sediments older than about 10 Ma have somewhat shallower patterns (excluding Ce) than those in Figure 3, suggesting that diagenetic effects have led to a loss in *HREE* relative to *LREE* (Barrett & Jarvis 1988). Slowly accumulating sediments deposited below the lysocline also show these effects, together with significant *REE* enrichment (Fig. 3). Eocene–Oligocene sediments from Sites 573 and 574 display even flatter patterns, consistent with further diagenetic fractionation of *REE*. Such near-flat patterns also characterize surface sediments affected by early diagenesis on the eastern flank of the EPR (Piper & Graef 1974) and in the Bauer Deep (Elderfield *et al.* 1981).

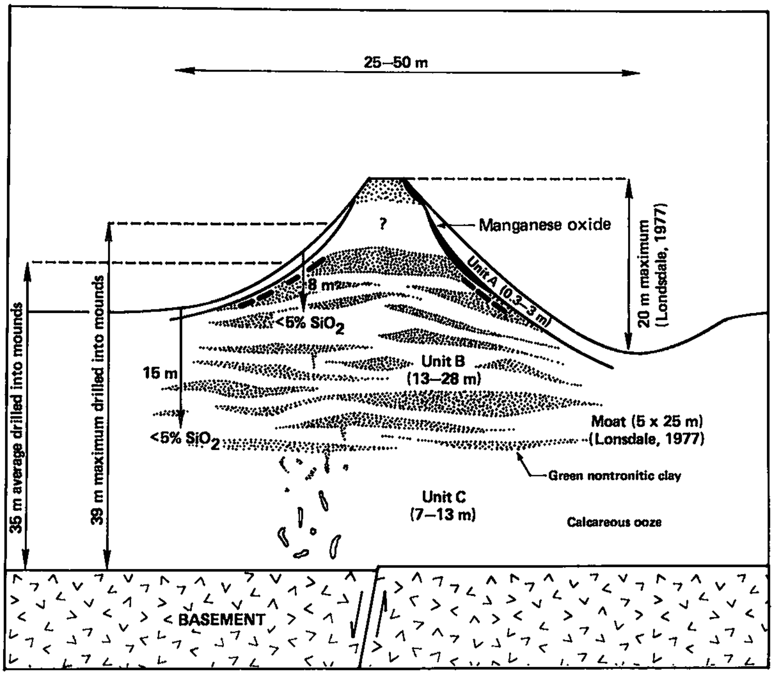

FIG. 4. Schematic diagram of the internal features and dimensions of a typical mound in the Galapagos hydrothermal mounds area (from Honnorez *et al.* 1981). Unit A is a thin surficial layer of calcareous pelagic ooze with local concentrations of Mn oxide plates, Unit B is a zone of interlayered beds of nontronite granules and normal pelagic ooze, and Unit C is pelagic ooze containing common nontronitic mottles that may mark the paths of upwelling hydrothermal solutions.

THE GALAPAGOS HYDROTHERMAL MOUNDS

In the Galapagos mounds area, located 18–32 km south of the Galapagos Rift in the eastern Pacific (Fig. 1), unusual Fe- and Mn-enriched sediments are present (Lonsdale 1977, Hékinian *et al.* 1978, Corliss *et al.* 1979, Natland *et al.* 1979). These sediments overlie young basement ≈0.5–0.9 Ma old, and occur within mound structures aligned parallel to basement faults; chains of mounds are typically separated by 100–200 m. The detailed stratigraphy of the mounds, which are typically 30-35 m thick, has been determined by piston coring during DSDP Leg 70 (Honnorez *et al.* 1981, 1983a). A schematic cross-section of a typical mound is shown in Figure 4. The main metalliferous component of the mounds is nontronite, an Fe-rich, Al-poor smectite that occurs as unconsolidated granules (≈90%) and muds in layers up to a few meters in thickness. Between this material and normal calcareous ooze which constitutes the background pelagic sediment, are transitional intervals of compact nontronitic mud. Manganiferous material, represented by crusts of Mn oxide and minor amounts of Mn–Fe oxide mud, is restricted to the upper 1-2 m of the mounds (Honnorez *et al.* 1981, Lalou *et al.* 1983). Pre-existent pelagic sediment apparently has been dissolved during nontronite formation (Moorby 1983), but there is also evidence that some biogenic material was replaced by nontronite (Borella *et al.* 1983). The upwelling solutions generally were not warmer than a few tens of degrees (Barrett *et al.* 1982). Nontronite and Mn oxide crust formed within the last few hundred Ka and few tens of Ka, respectively (Lalou *et al.* 1983). We have further investigated nontronite formation by analyzing splits of granular and transitional-zone nontronite for oxygen isotopes, *REE*, and Pb isotopes.

Sample material and mineralogy

Typical core samples of granular and transitional-zone nontronite are shown in Figure 5. The granules (top of Fig. 5a) are typically dark green and 2–10 mm in diameter; although firm in consistency, they can be broken by hand to clay-size particles. In the transitional intervals between this lithology and whitish nannofossil ooze, the nontronite is fine-grained, compact and light green (Fig. 5b). Small enclaves of pelagic sediment surrounded by nontronite are locally present (Fig. 5a). Mn–Fe-oxide mud, present only in Hole 509B, occurs as two layers ≈10 cm thick near the top of the hole. The mud is brownish black and gelatinous, and consists dominantly of Mn-oxide microaggregates.

X-ray diffraction study of splits was carried out for all samples. The powders were untreated and randomly oriented, and were run using Co*K*α radiation

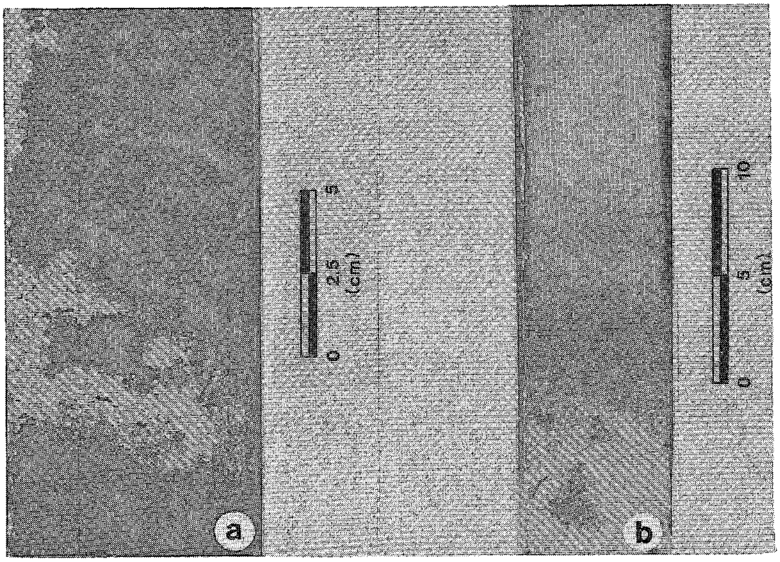

FIG. 5. Typical examples of granular and transitional-zone nontronite from the Galapagos mounds (Honnorez *et al.* 1983b). (a): Granular nontronite with a residual enclave of mottled calcareous ooze; (b): granular nontronite (top) showing a smooth gradation over ≈20 cm through fine-grained, compact, transitional-zone nontronite, to normal calcareous ooze.

(50 kV, 20 mA) at a scan speed of 1° 2θ min^{-1}. The results indicate that a single near-uniform nontronitic phase dominates the sediments, with minor to trace amounts of calcite, and traces of quartz. Although the term "nontronite" has been conventionally used for this phase, detailed XRD and chemical studies indicate that it typically consists of disordered, mixed-layer, nontronite–celadonite with a dioctahedral structure (Honnorez *et al.* 1983a, Varentsov *et al.* 1983, McMurtry *et al.* 1983). In the present sample set, the major peaks are, in order of decreasing intensity: 4.51–4.54, 10.0–10.3, 2.56–2.60, 4.35–4.40, ≈3.25–3.35, 1.51–1.52, and 2.39–2.46 Å.

Composition

The chemical composition of five nontronitic samples analyzed by X-ray fluorescence is given in Table 1 (analyses done at McGill University on sample splits of initial 10–20 cc samples). The limited range in major-element composition is consistent with previous studies (Corliss *et al.* 1978, Hékinian *et al.* 1978, Migdasov *et al.* 1983, Moorby 1983, McMurtry *et al.* 1983). Excluding sample 509B-1-2, which contains minor Mn oxides, the nontronitic material has a Fe_2O_3/SiO_2 ratio of 0.54 to 0.60. This was also the range found for individual granules from different mounds (Barrett *et al.* 1982). The proportions of Mg and alkalis to SiO_2 are also fairly uniform. The concentrations of Al_2O_3 are commonly <0.5%, indicating that detrital phases are almost absent. The cited studies show that there are no significant variations in the major-element composition of nontronite that might explain the ranges in *REE* composition and in Pb isotopic ratios (see below). These studies also indicate that the nontronitic intervals have much lower trace-element contents (*e.g.*, Cu, Pb, Zn) than the Fe–Mn oxyhydroxide sediments discussed earlier.

TABLE 2. OXYGEN ISOTOPIC COMPOSITION OF METALLIFEROUS SEDIMENTS FROM DSDP LEG 70 AND ESTIMATED TEMPERATURES OF FORMATION OF NONTRONITE

Sample	Nature of Sediment	$\delta^{18}O$	T (C°)
506-6-2: 24-25 cm	Slightly granular nontronite	24.8	27
506-6-2: 65-67 cm	Granular nontronite	25.9	21
506C-2-1: 35-36 cm	Transitional nontronite with Fe-Mn oxide mud	14.0	
506C-3-3: 100-102 cm	Granular nontronite	11.2	137
506C-4-2: 92-93 cm	Slightly granular nontronite	26.3	19
506D-2-3: 79-80 cm	Transitional nontronite, off-mounds (CF)	18.2	
507D-6-2: 85-86 cm	Granular nontronite	26.3	19
507D-6-2: 130-132 cm	Granular nontronite	26.2	19
507D-6-3: 30-31 cm	Transitional nontronite	22.4	
509B-1-1: 112-113 cm	Gelatinous mud; oxides present	≈6	
509B-1-2: 124-125 cm	Granular nontronite (CF) minor Mn oxides	26.4	21 (max)
509B-2-1: 119-120 cm	Gelatinous mud; Fe-Mn oxides present	8.3	
509B-3-1: 142-144 cm	Granular nontronite	28.6	9
509B-3-2: 58-59 cm	Transitional nontronite	23	
509B-4-1: 140-142 cm	Transitional nontronite	23	
509B-5-2: 29-30 cm	Nontronitic mottle (CF) (subsample)	23 25	36 26

$\delta^{18}O$ values in per mil relative to Standard Mean Ocean Water. Temperatures were calculated using the smectite geothermometer of Savin (pers. comm. 1988), revised after Yeh & Savin (1977). Three samples (CF) were treated with dilute hydrochloric acid prior to analysis to remove carbonate ooze.

TABLE 3. Pb ISOTOPIC DATA FOR METALLIFEROUS SEDIMENTS FROM THE GALAPAGOS HYDROTHERMAL MOUNDS

Sample	$^{206}Pb/^{204}Pb$	$^{207}Pb/^{204}Pb$	$^{208}Pb/^{204}Pb$
506-6-2: 24-25	18.604 ± 0.017	15.608 ± 0.018	38.403 ± 0.049
506-6-2: 130-132	18.900 ± 0.031	15.638 ± 0.026	38.645 ± 0.072
506C-2-1: 35-36	18.745 ± 0.011	15.583 ± 0.012	38.543 ± 0.043
506C-3-3: 100-102	19.080 ± 0.015	15.655 ± 0.013	38.586 ± 0.046
506C-4-2: 92-93	18.711 ± 0.011	15.613 ± 0.013	38.641 ± 0.040
506D-2-3: 79-80	18.918 ± 0.011	15.646 ± 0.012	38.795 ± 0.040
507D-6-2: 85-86	19.092 ± 0.011	15.665 ± 0.013	38.738 ± 0.040
507D-6-3: 30-31	18.590 ± 0.015	15.636 ± 0.016	38.426 ± 0.046
509B-1-2: 124-125	18.861 ± 0.011	15.648 ± 0.014	38.487 ± 0.040
509B-2-1: 119-120	18.975 ± 0.016	15.677 ± 0.020	38.776 ± 0.054
509B-4-1: 140-142	18.802 ± 0.011	15.632 ± 0.013	38.676 ± 0.041
509B-5-2: 29-30	18.865 ± 0.014	15.645 ± 0.017	38.672 ± 0.047

Uncertainties are quoted at the 95% confidence level.
Sample lithologies given in Table 2.

Oxygen isotopes

The oxygen isotope composition of the metalliferous sediments, together with the temperatures of nontronite crystallization estimated using the geothermometer of Yeh & Savin (1977), are given in Table 2. Most of the temperatures are in the 19–36°C range, although one low value of 9°C, and one much higher value of 137°C were obtained. The range is similar to that obtained on carbonate-free, nontronitic bulk samples from Leg 70 (19–32°C: Barrett & Friedrichsen 1982), and on the chemically purified, <0.2 μm fraction of nontronitic clays from the Galapagos mounds field (25–47°C: McMurtry *et al.* 1983). Temperatures are close to those estimated for the basalt–sediment contact on the basis of heat-flow data (Becker *et al.* 1983). Temperatures were not calculated for the transitional-zone nontronite because chemical data (Moorby 1983) indicate that detrital material is present in these layers.

According to the models of Fehn (1986), narrow, off-axial zones of hydrothermal discharge exist that do not move away from the spreading axis as the crust recedes. The models predict a first discharge phase (<200°C) at about 16 km from the Galapagos axis, with a second possible phase located beyond the limit of the mound field drilled on Leg 70. Of the three mounds drilled on Leg 70, all presently characterized by low temperatures, Site 506 is the closest to the ridge axis (≈22 km away, on crust ≈630 Ma old). At hole 506C, both high-temperature (one sample) and low-temperature nontronite occur within one mound (Table 2). By contrast, at Sites 507 and 509, located on crust ≈750 Ma and ≈900 Ma old, nontronite formation may have taken place over longer intervals within the low-temperature regime. Although more data are required, we favor a model wherein initial formation of nontronite on a significant scale occurs above the first zone of off-axial basement discharge, so that at least some nontronite forms at higher temperatures (perhaps 50–150°C). Continued growth of nontronite with recession of the crust leads to more and more low-temperature nontronite. Thus most bulk samples will eventually attain isotopic compositions corresponding to the average temperature regime that has existed over the last few hundred thousand years, which apparently was less than ≈40°C.

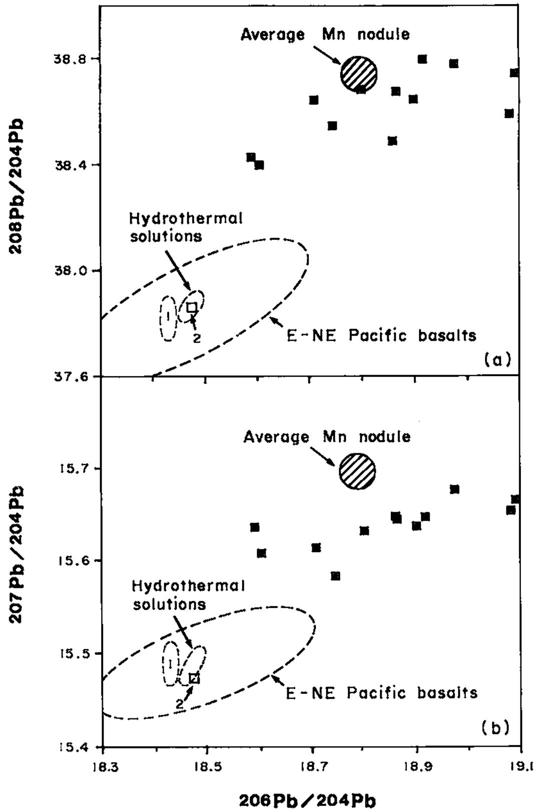

FIG. 6. Pb isotope data for metalliferous sediments (mostly nontronite samples) from the Galapagos hydrothermal mounds, DSDP Leg 70. Sources of data for Mn nodules and Pacific basalts as in Figure 2. The small oval (1) represents the least radiogenic end-member composition of Leg 92 metalliferous sediments (Fig. 2). Box 2 is the average composition of massive sulfides (Fig. 2); the field marked "hydrothermal solutions" encloses the range in Pb isotopic compositions of high-temperature solutions at 21°N EPR and the Juan de Fuca Ridge (Chen 1987).

Pb isotopes

The Pb isotopic composition of nontronitic sediments is given in Table 3 and plotted in Figure 6. The data partly overlap with, but are generally more radiogenic than samples analyzed by Barrett & Friedrichsen (1982) from the same mounds. In that study, the Pb isotopic composition of some of the nontronite samples was interpreted as a mixture of basalt-derived and seawater Pb, as for the Leg 92 samples. Although some of the new samples apparently contain mixtures of basaltic and seawater Pb, many are more radiogenic than seawater, for which there is no obvious explanation (in the earlier study, two such radiogenic nontronite samples were found). Replacement of local pelagic sediment by nontronite is unlikely to produce the radiogenic values because $^{206}Pb/^{204}Pb$ ratios of the former do not exceed 18.7 (Barrett & Friedrichsen 1982). A possible source for the radiogenic Pb is certain volcanic rocks of the Galapagos Islands (White 1979), although their Pb isotopic ratios do not exactly match those of the anomalous nontronite. Minor disseminated volcanic ash occurs in the normal pelagic sediments that surround the hydrothermal mounds, and several discrete ash beds a few cm thick are present in the sediment column (Honnorez *et al.* 1983b). Although the composition of such ash is unknown, glass shards replaced by nontronite (which have been observed) may have retained radiogenic Pb. Studies of ash layers are planned to test this possibility.

Rare-earth elements

Most nontronitic sediments from the Galapagos mounds area (Table 4, Fig. 7) have *REE* concentrations significantly lower than those of typical shale, with relative *HREE* enrichment (see also Bonnot-Courtois 1981, and Migdisov *et al.* 1983). The nontronite *REE* patterns are similar to those of deep seawater in the eastern Pacific (De Baar *et al.* 1985), although Ce anomalies are notably less negative than that of seawater.

Nontronite from the transitional zones has the highest *REE* concentrations, and very similar patterns (top two patterns in each of Figs. 7a,b). Gelatinous mud has the next highest *REE* concentrations, and almost identical patterns (two middle patterns in Fig. 7b). Slightly granular nontronite has intermediate *REE* concentrations (three middle pat-

TABLE 4. RARE EARTH ELEMENT COMPOSITION OF METALLIFEROUS SEDIMENTS FROM DSDP LEG 70

REE ppm	506-6-2: 24-25 cm	506-6-2: 65-67 cm	506-7-1: 95-97 cm	506C-2-1: 35-36 cm	506C-3-3: 100-102 cm	506C-4-2: 92-93 cm	506D-2-3: 79-80 cm
La	4.31	0.94	4.98	17.4	1.39	3.32	14.3
Ce	4.07	0.70	5.76	16.1	1.76	2.34	19.2
Pr	0.98	b.d.	0.95	3.58	b.d.	b.d.	3.37
Nd	4.14	0.74	3.59	14.7	1.00	2.29	13.1
Sm	0.88	0.17	0.83	3.31	0.29	0.66	2.88
Eu	0.21	0.05	0.20	1.00	0.07	0.16	0.77
Gd	1.13	0.20	0.92	4.18	0.29	0.74	3.59
Dy	1.24	0.20	0.98	4.28	0.25	0.94	3.11
Ho	0.27	0.06	0.20	0.88	0.06	0.20	0.65
Er	0.92	0.22	0.61	2.90	0.20	0.60	2.08
Yb	0.96	0.26	0.73	2.98	0.26	0.69	2.16
Lu	0.15	0.05	0.13	0.47	0.05	0.11	0.34
Y	14.0	2.62	8.78	32.2	2.06	7.32	21.5

REE ppm	507D-6-2: 85-86 cm	509B-1-1: 112-113 cm	509B-1-2: 124-125 cm	509B-2-1: 119-120 cm	509B-3-2: 58-59 cm	509B-4-1: 140-142 cm	509B-5-2: 29-30 cm	SCo-1 standard
La	1.89	8.33	0.86	7.97	12.8	15.2	1.02	29.9
Ce	2.35	7.89	0.82	6.56	14.9	20.3	1.31	58.6
Pr	b.d.	1.76	b.d.	1.28	1.94	4.17	b.d.	7.32
Nd	1.15	6.72	0.93	5.83	12.4	18.2	0.80	26.3
Sm	0.34	1.56	0.17	1.31	3.03	4.46	0.16	5.02
Eu	0.08	0.43	0.04	0.35	0.86	1.27	0.06	1.12
Gd	0.31	1.91	0.21	1.79	3.47	5.02	0.25	4.12
Dy	0.32	1.94	0.31	1.94	3.62	5.19	0.26	3.35
Ho	0.07	0.38	0.06	0.39	0.75	1.05	0.06	0.64
Er	0.25	1.27	0.18	1.20	2.33	2.99	0.18	1.81
Yb	0.24	1.36	0.20	1.34	2.15	2.66	0.23	1.83
Lu	0.04	0.22	0.03	0.20	0.35	0.42	0.03	0.28
Y	2.67	14.1	1.86	14.9	24.8	36.1	2.95	18.1

b.d. = below detection
Sediment types given in Table 2

terns in Fig. 7a); two of the patterns are very similar. Granular nontronite has the lowest *REE* concentrations (lowest two patterns in Fig. 7a, and lowest three in Fig. 7b). No stratigraphic variations in *REE* concentration or pattern are discernible. Almost identical concentrations and patterns were obtained for both the shallowest and the deepest samples of granular nontronite (509B-1-2 and 506-6-2, respectively).

The passage from transitional (506-6-2: 24–25 cm) to granular nontronite (506–6-2: 65–67 cm) within a single nontronitic bed is accompanied by a 5-fold decrease in *REE* concentration, and by a modest increase in the ratio of *HREE* to *LREE* (Fig. 7a). In one thick bed of granular nontronite, three samples within an 85-cm interval have very low *REE* concentrations (507D-6-2: 65–67 cm, and 2 samples below detection limits). These data indicate that the development of nontronite, from transitional to slightly granular to coarsely granular, is accompanied by reduction in *REE* concentrations. We speculate that this reflects rejection of *REE* from increasingly crystalline nontronite (preliminary XRD data do not allow assessment of this). Variations in the *REE* profiles of nontronite cannot be explained on the basis of bulk chemical variations, as nontronite granules are compositionally near-uniform.

REE patterns for nontronite are distinct from those of high-temperature vent waters at the EPR (Michard *et al.* 1983), metalliferous sediment from the eastern Pacific (Barrett & Jarvis 1988), and basalt underlying the mounds at Sites 506 and 507 (Emmerman *et al.* 1983). Most of the *REE* in nontronite probably are inherited from pore waters or from dissolution of carbonate ooze. Because the *REE* abundances of carbonate tests are several orders of magnitude higher than concentrations in seawater (Elderfield *et al.* 1981), dissolved carbonate ooze is a more likely source of seawater *REE*. The less negative Ce anomalies of nontronite may reflect precipitation from pore waters that were less oxidized than normal seawater (allowing some Ce^{3+} to remain in solution). Alternatively, a minor basaltic component in nontronite bulk samples could make the Ce anomaly less negative than that of seawater. No nontronite samples display a positive Eu anomaly, which typifies most chemical sediments in the brine deeps of the Red Sea (Courtois & Treuil 1977, Oudin & Cocherie 1988). This indicates that the pore waters from which nontronite formed were not strongly reducing.

Hydrothermal mounds such as those in the Galapagos field are probably uncommon. Development of mounds apparently requires a high rate of biogenic sedimentation, such as occurs under the equatorial high-productivity belt, together with an

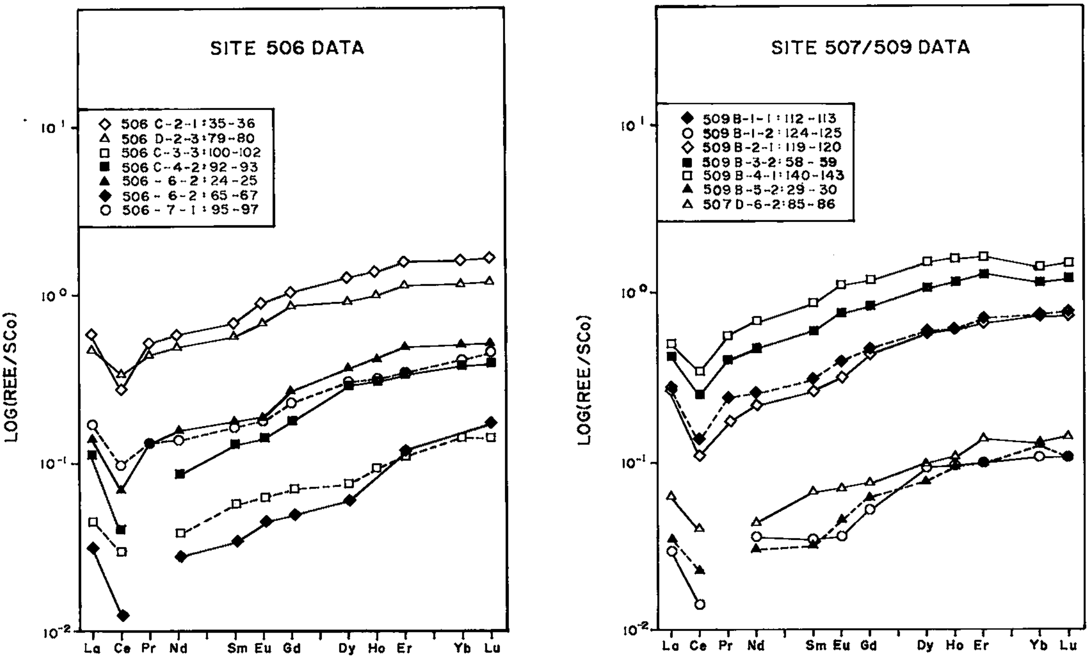

FIG. 7. *REE* patterns for metalliferous sediments (mostly nontronite samples) from the Galapagos hydrothermal mounds, DSDP Leg 70. All samples have distinctly less negative Ce anomalies than Leg 92 sediments (Fig. 3) or deep seawater in the eastern Pacific (De Baar *et al.* 1985).

off-axial location and a moderate spreading rate. As a result, relatively low-temperature, upwelling solutions are forced to pass through and react with a sediment cover which blankets basement topography. In response to progressive oxidation of upwelling solutions, precipitation of Fe^{2+} and Si as Fe^{3+}-rich nontronite occurs in the upper levels of the mounds, followed by precipitation of Mn^{2+} as Mn^{4+}-rich oxides close to the sediment surface (*cf.* Corliss *et al.* 1978, Dymond *et al.* 1980, Hékinian *et al.* 1980). Some of the Si may be derived from the dissolution of pelagic ooze that accompanies nontronite formation (Honnorez *et al.* 1981). The experiments of Harder (1976) indicate that a slightly reducing solution with low Mg and Al contents favors formation of nontronite over other smectite minerals.

MASSIVE SULFIDE GOSSANS ON THE SOUTHERN EXPLORER RIDGE

Five gossan samples from the Southern Explorer Ridge median valley in the northeast Pacific were obtained by the PISCES IV submersible during the CASM IV cruise (Scott *et al.* 1984). Within the eastern part of the median valley, some two dozen massive sulfide deposits form mound-like edifices some 10 to 200 m in length. Except for one mound locally venting water at ≈25°C (dive P1505), all others are presently inactive. On the surface of the mounds, bright orange- to red-brown sediments up to several cm thick are draped over and surround rubble and blocks of rusty sulfate-bearing sulfides up to a meter in size (see also Francheteau *et al.* 1979, Oakman & Leinen 1985, Alt *et al.* 1987). These distinctively colored oxidized sediments are also observed up to about 100 m from the sulfide deposits. The massive deposits consist of finely intermixed zinc sulfide, iron sulfides, barite and chalcopyrite. Three gossan samples were from the Thruster sulfide deposit, one of the largest in the area, and all are from mounds between 49°43′ and 49°46′ N, and 130° 12′ and 130°19′ W. Two sediments overlying basalt were also included, one from the axial valley of the Southern Explorer Ridge (P1505-6), the other from the edge of the caldera at Axial Seamount (AX-1) (CASM 1985).

We analyzed the <200 mesh (<70μm) fraction of the sediments, which represents about 10–25% of the total sediment. Leach treatments indicate that the <200 mesh fraction consists of: 3–12% carbonate, 25–35% oxyhydroxides = leachable metalliferous component, and 50–70% residue (Table 5). Sample P1504-7 differs in having ≈75% metalliferous component. Coarser fractions contain foraminiferal and basaltic fragments in addition to hydrothermal material. XRD data for the <200

TABLE 5. COMPOSITION OF METALLIFEROUS COMPONENT OF INTRA-RIFT SEDIMENTS, SOUTHERN EXPLORER RIDGE --calculated on a salt-free carbonate-free basis, for the <200 mesh fraction--

															Bulk sample basis			
Sample	Leach	Al %	Mg %	K %	Ca %	Sr %	Fe %	Mn %	Cu %	Zn ppm	Pb ppm	Ni ppm	Co ppm	Si ppm	L-1 %	L-2 %	L-3 %	Res. %
P1505-13*	L-2	0.02	0.01	0.00	0.01	0.01	2.19	0.00	0.17	604	370	16	9	1960				
	L-3	0.11	0.08	0.01	0.08	0.32	1.53	0.01	0.92	737	307	13	34	673				
	Total	0.13	0.09	0.01	0.09	0.33	3.72	0.01	1.09	1341	677	29	43	2633	2.5	6.4	17.4	73.8
P1505-14*	L-2	0.02	0.01	0.00	0.03	0.01	4.79	0.00	0.13	577	553	16	9	4760				
	L-3	0.08	0.05	0.01	0.08	0.32	6.73	0.01	0.54	478	475	12	32	2480				
	Total	0.10	0.06	0.01	0.11	0.33	11.52	0.01	0.67	1055	1028	28	41	7240	4.5	10.9	22.6	62.0
P1505-15*	L-2	0.02	0.01	0.00	0.02	0.01	4.31	0.00	0.13	526	524	16	9	4325				
	L-3	0.07	0.06	0.01	0.08	0.34	2.38	0.01	0.61	590	340	28	31	1300				
	Total	0.09	0.07	0.01	0.10	0.35	6.69	0.01	0.74	1116	864	44	40	5625	3.0	9.9	18.5	68.6
P1506-5#	L-2	0.11	0.04	0.01	0.10	0.01	1.36	0.11	0.08	249	157	32	18	2620				
	L-3	1.42	0.74	0.09	0.96	0.23	2.47	0.02	0.32	302	164	54	44	1200				
	Total	1.53	0.78	0.10	1.06	0.24	3.83	0.13	0.40	551	321	86	62	3820	5.3	9.5	18.8	66.5
P1504-7*	L-2	0.02	0.08	0.00	0.15	0.01	11.30	0.07	1.63	533	304	16	13					
	L-3	0.24	0.14	0.03	0.11	0.03	28.80	0.01	1.12	634	505	44	75					
	Total	0.26	0.22	0.03	0.26	0.04	40.10	0.08	2.75	1167	809	60	88		8.0	22.8	52.5	16.7
AX-1#	L-2	0.46	0.23	0.03	0.42	0.01	1.98	0.54	0.00	36	19	25	11					
	L-3	5.66	2.95	0.16	5.15	0.01	7.21	0.10	0.01	97	98	90	60					
	Total	6.12	3.18	0.19	5.57	0.02	9.19	0.64	0.01	133	117	115	70		12.4	6.1	30.5	51.0
P1502-7*	L-2	0.16	0.11	0.02	0.17	0.01	2.94	2.90	0.03	231	145	76	10					
	L-3	2.18	0.99	0.21	0.50	0.03	4.67	0.11	0.21	251	70	58	45					
	Total	2.34	1.10	0.23	0.67	0.04	7.61	3.01	0.24	482	215	134	55		8.6	13.3	19.2	58.9

*Sediment from gossans overlying inactive sulfide mounds. #Sediment overlying basalt.

mesh fraction of the gossans indicate that the leachable metalliferous component consists mainly of goethite and barite (amorphous oxyhydroxides and phases below detection limits could also be present), whereas the residue is mainly barite.

Chemical composition. On a carbonate- and salt-free basis, the leachable metalliferous component (L-2 + L-3 in Table 5) contains 7.6 to 40% Fe and up to 3% Mn. Contents of Ca, Mg and Al, elements typically associated with siliciclastic phases, are generally less than 1–2% except in the Axial Seamount sample. Leachable material can be divided into three groups (Figs. 8a–c): 1) Mn-poor sediments (Mn ≈0.01%) with high Cu and Sr contents (Cu/Mn and Sr/Mn ≈75 and 30, respectively). These samples are all from the large Thruster sulfide deposit. 2) Intermediate sediments with Mn ≈0.1%, from the surface of mound P1504, and overlying basalt on the eastern propagator of the SER axis. 3) Mn-rich sediments (Mn = 0.6–3.0%) from the Axial Seamount caldera and the surface of mound P1502. These sediments are also rich in Ca + Mg + Al, suggesting the presence of altered (= leachable) volcaniclastic material, but are poor in Sr and Cu. For the mound sediment, Cu/Mn and Sr/Mn ratios (≈0.1 and 0.01, respectively) are some three orders of magnitude less than in the first group.

General hypothesis. The above data, together with the tendency for Mn to be enriched in low-temperature hydrothermal precipitates near discharge sites (Scott *et al.* 1974, Rona 1980, Moorby 1983), allow inference of the following processes during ageing of sulfide/sulfate deposits on the seafloor. The exposure time of axial deposits probably varies considerably depending on sedimentation rate, duration of volcanic activity, and tectonic effects.

1) *In situ* oxidation of massive sulfides and sulfates exposed to cold seawater at the surfaces of the mounds (*e.g.*, Oakman & Leinen 1985) produces a thin, surficial blanket of gossan. The alteration product consists mainly of Fe oxyhydroxide phases, with Fe/Mn ratios of ≈200–1000. Leachable sediments of the first type (Fig. 8a) would represent this category, and presumably reflect the composition of the initial sulfide/sulfate material, with high Cu and Sr concentrations (the latter due to sulfates), low Mn of ≈100 ppm, and low Ca + Mg + Al of ≈1000 ppm (almost no altered volcaniclastic material). Support for the young age of the Thruster gossans is provided by their location only a few hundred meters from Magic Mountain, the main site of present high-temperature hydrothermal activity (axial deposits to the south are inactive). Fe oxyhydroxide sediments need not be formed entirely through oxidation of sulfides; for example, on Red Seamount at the EPR, Fe oxyhydroxides are precipitating directly from low-temperature (10–15°C) hydrothermal solutions (Alt *et al.* 1987).

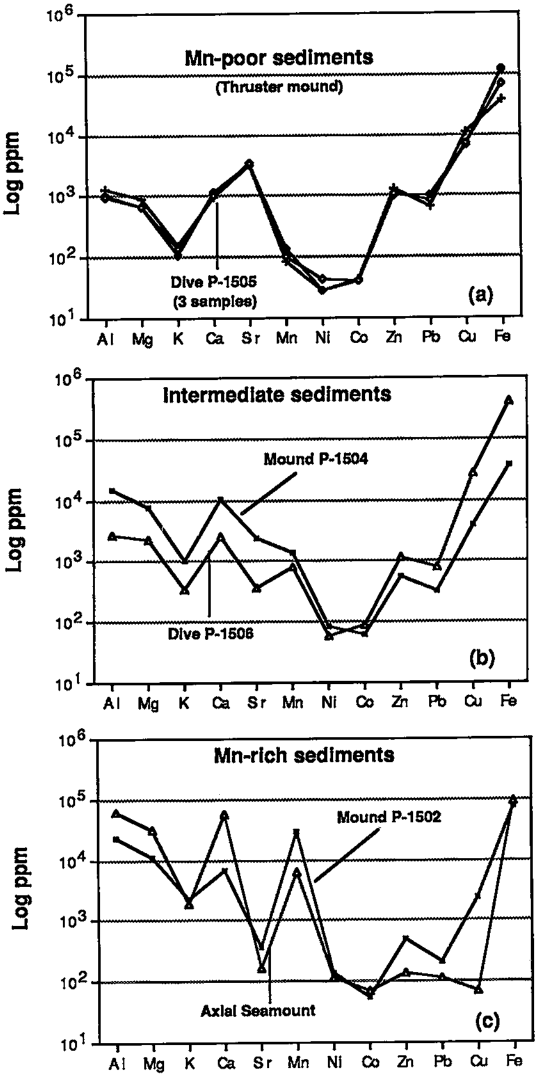

FIG. 8. Elemental composition plots for the leachable component of five gossans overlying sulfide/sulfate mounds in the axial valley of the Southern Explorer Ridge (sites 1505, 1504 and 1502), and of the leachable component of sediment overlying basalt in this valley (site 1506) and at Axial Seamount (Fig. 8c).

2) If volcanic activity in the environment is dispersing basaltic glass fragments (*cf.* Bonatti 1970), these may become incorporated into the gossan. The presence of basaltic alteration products (*e.g.*, palagonite) could account for the increased Ca + Mg + Al values in the leachates. With time, hydrothermal Mn derived from active vents elsewhere on the axis (*cf.* Klinkhammer & Bender 1980) is scavenged by the particulate Fe oxyhydroxide phases (*cf.* Weiss *et al.* 1977). Leachable sediments of the second type (Fig. 8b) constitute this category.

3) With continued exposure of the gossans, the low-temperature hydrothermal Mn contribution increases through further scavenging, and the altered volcaniclastic component may increase. Sample P1502-7 of the third category (Fig. 8c) has the highest Mn and Ca + Mg + Al values. The overall elemental distribution in the leachable fraction of this sample is very similar to that of Cyprus umber (Robertson 1986). The Axial Seamount sample, which does not overlie a sulfide mound but overlies basalt at the edge of the caldera, has much lower metal contents (excluding Mn). The high ratio of Mn to (Zn + Cu + Pb) suggests a near-vent, low-temperature hydrothermal component similar to that in the TAG geothermal area of the Mid-Atlantic Ridge (Scott *et al.* 1974, Shearme *et al.* 1983).

Comment

The sulfide mounds underlying the gossans initially could have contained a component of hydrothermal smoke particles, as most particles larger than ≈ 100 μm should fall within a few hundred meters of the vents (Feely *et al.* 1987). Sulfide particles smaller than ≈ 30 μm should be dispersed farther than a few km from the vents (Converse *et al.* 1984). However, it is unlikely that smoke particles are deposited in sulfide form at distances of even a few km. Metalliferous sediments as close as 10 km to the EPR axis consist mainly of Fe–Mn oxyhydroxides (Marchig & Erzinger 1986), and even sediments within tens of m of vents on the Juan de Fuca Ridge contain no sulfide material (Leinen 1986). The discovery of Fe–Mn oxyhydroxide particulates as the main phase in plumes above high-temperature vents (*e.g.*, the Juan de Fuca Ridge: Baker *et al.* 1985, Baker & Massoth 1987, Feely *et al.* 1987) suggests that direct precipitation of oxyhydroxides and oxidation of sulfide particles both begin very soon after hydrothermal discharge.

ACKNOWLEDGEMENTS

We are indebted to the Deep Sea Drilling Project and the curatorial staff for their assistance during post-cruise sampling of Leg 70 and Leg 92 cores. We thank Drs. R.L. Chase and S.D. Scott, and the scientific and ship's crews of the CASM IV cruise. Joanna Lugowski conducted sample preparation and analysis at the University of Toronto. Additional analytical facilities were provided by the City of London Polytechnic and the University of Alberta. We thank Ian Hutcheon, J. Adshead, and two anonymous reviewers of earlier portions of this paper for their constructive comments. This research was supported by grants from the Natural Sciences and Engineering Research Council of Canada (T.J.B., F.J.L. and R.F.), and by Kingston Polytechnic, G.B. (I.J.).

REFERENCES

Aoki, S., Kohyama, N. & Sudo, T. (1974): An iron-rich montmorillonite in a sediment core from the northeastern Pacific. *Deep-Sea Res.* **21**, 865-875.

Alt, J.C., Lonsdale, P., Haymon, R. & Muehlenbachs, K. (1987): Hydrothermal sulfide and oxide deposits on seamounts near 21°N, East Pacific Rise. *Geol. Soc. Amer. Bull.* **98**, 157-168.

Bäcker, H., Lange, J. & Marchig, V. (1985): Hydrothermal activity and sulphide formation in axial valleys of the East Pacific Rise crest between 18 and 22°S. *Earth Planet. Sci. Lett.* **72**, 9-22.

Baker, E.T., Lavelle, J.W. & Massoth, G.J. (1985): Hydrothermal particulate plumes over the southern Juan de Fuca Ridge. *Nature* **316**, 342-344.

——— & Massoth, G.J. (1987): Characteristics of hydrothermal plumes from two vent fields on the Juan de Fuca Ridge, northeast Pacific Ocean. *Earth Planet. Sci. Lett.* **85**, 59-73.

Barrett, T.J. & Friedrichsen, H. (1982): Elemental and isotopic composition of some metalliferous and pelagic sediments from the Galapagos mounds area, DSDP Leg 70. *Chem. Geol.* **36**, 275-298.

——— & Jarvis, I. (1988): Rare earth element geochemistry of metalliferous sediments from DSDP Leg 92: the East Pacific Rise transect. *Chem. Geol.* **67**, 243-259.

———, Taylor, P.N. & Lugowski, J. (1987): Metalliferous sediments from DSDP Leg 92: The East Pacific Rise transect. *Geochim. Cosmochim. Acta* **51**, 2241-2253.

———, ———, Jarvis, I. & Lugowski, J. (1986): Pb and Sr isotope and rare earth element composition of selected metalliferous sediments from Sites 597 to 601, Deep Sea Drilling Project Leg 92. *Initial Reports Deep Sea Drilling Project* **92**, 391-407. U.S. Gov. Printing Office, Washington, D.C.

Becker, K., Von Herzen, R.P. & Karato, S. (1983): Geothermal measurements from drilling of sediments near the Galapagos Spreading Center 86°W, Deep Sea Drilling Project Leg 70. *Initial Reports Deep Sea Drilling Project* **70**, 445-458. U.S. Gov. Printing Office, Washington, D.C.

Bender, M.L., Broecker, W., Gornitz, V., Middel, U., Kay, R., Sun, S.S. & Biscaye, P. (1971): Geochemistry of three cores from the East Pacific Rise. *Earth Planet. Sci. Lett.* **12**, 425-433.

Bonatti, E. (1970): Deep sea volcanism. *Naturwiss.* **57**, 379-384.

Bonnot-Courtois, C. (1981): Distribution des terres rares dans les dépôts hydrothermaux de la zone FAMOUS et des Galapagos – Comparaison avec des sédiments métallifères. *Mar. Geol.* **39**, 1-14.

Borella, P.E., Myers, R. & Mills, B. (1983): Sediment petrology of the hydrothermal mounds. *Initial Reports Deep Sea Drilling Project* **70**, 197-209. U.S. Gov. Printing Office, Washington, D.C.

Boström, K. & Peterson, M.N.A. (1966): Precipitates from hydrothermal exhalations on the East Pacific Rise. *Econ. Geol.* **61**, 1258-1265.

———, ———, Joensuu, O. & Fisher, D.E. (1969): Aluminum-poor ferromanganoan sediments on active oceanic ridges. *J. Geophys. Res.* **74**, 3261-3270.

Brevart, O., Dupré, B. & Allègre, C.J. (1981): Metallogenesis at spreading centers: Lead isotope systematics for sulfides, manganese-rich crusts, basalts, and sediments from the CYAMEX and ALVIN areas (East Pacific Rise). *Econ. Geol.* **76**, 1205-1210.

Burke, W.A., Denison, R.E., Hetherington, E.A., Koepnick, R.B., Nelson, H.F. & Otto, J.B. (1982): Variation of seawater ^{87}Sr/^{86}Sr throughout Phanerozoic time. *Geology* **10**, 516-519.

CASM (1985): Hydrothermal vents on an axis seamount of the Juan de Fuca Ridge. *Nature* **313**, 212-214.

Chen, J.H. (1987): U, Th, and Pb isotopes in hot springs on the Juan de Fuca Ridge. *J. Geophys. Res.* **92**, 11411-11415.

———, Wasserburg, G.J., Von Damm, K.L. & Edmond, J.L. (1986): The U-Th-Pb systematics in hot springs on the East Pacific Rise at 21°N and Guaymas Basin. *Geochim. Cosmochim. Acta* **50**, 2467-2479.

Chester, R. & Hughes, M.J. (1967): A chemical technique for the separation of ferromanganese minerals, carbonate minerals and adsorbed trace elements from pelagic sediments. *Chem. Geol.* **2**, 249-262.

Church, S.E. & Tatsumoto, M. (1975): Lead isotope relations in oceanic ridge basalts from the Juan de Fuca – Gorda Ridge area, N.E. Pacific Ocean. *Contrib. Mineral. Petrology* **53**, 253-279.

Circum-Pacific Council for Energy and Mineral Resources (1981): Plate-Tectonic Maps of the Circum-Pacific Region, Northwest Quadrant. *Amer. Assoc. Petrol. Geol.*, Tulsa, U.S.A.

Clayton, R.N. & Mayeda, R.K. (1963): The use of bromine pentafluoride in the extraction of oxygen from oxides and silicates for isotopic analysis. *Geochim. Cosmochim. Acta* **27**, 43-52.

Cole, T.G. (1985): Composition, oxygen isotope geothermometry, and origin of smectite in the metalliferous sediments of the Bauer Deep, southeast Pacific. *Geochim. Cosmochim. Acta* **49**, 221-235.

Converse, D.R., Holland, H.D. & Edmond. J.M. (1984): Flow rates in the axial hot springs of the East Pacific Rise (21°N): implications for heat budget and the formation of massive sulphide deposits. *Earth Planet. Sci. Lett.* **69**, 159-175.

Corliss, J.B., Dymond, J., Gordon, L.I., Edmond, J.M., Von Herzen, R.P., Ballard, R.D., Green, K., Williams, D., Bainbridge, A., Crane K. & Van Andel, T.H. (1979): Submarine thermal springs on Galapagos Rift. *Science* **203**, 1073-1083.

———, Lyle, M., Dymond, J. & Crane, K. (1978): The chemistry of hydrothermal mounds near the Galapagos Rift. *Earth Planet. Sci. Lett.* **40**, 12-24.

Courtois, C. & Treuil, M. (1977): Distribution des terres rares et de quelques éléments en trace dans les sédiments récents des fosses de la Mer Rouge. *Chem. Geol.* **20**, 57-72.

Cronan, D.S. (1973): Basal ferruginous sediments cored during Leg 16, Deep Sea Drilling Project. *Initial Reports Deep Sea Drilling Project* **16**, 601-604. U.S. Gov. Printing Office, Washington, D.C.

——— (1976): Basal metalliferous sediments from the eastern Pacific. *Geol. Soc. Amer. Bull.* **87**, 928-934.

Dasch, E.J., Dymond, J.R. & Heath, G.R. (1971):

Isotopic analysis of metalliferous sediments from the East Pacific Rise. *Earth Planet. Sci. Lett.* **13**, 175-180.

De Baar, H.J.W., Bacon, M.P. & Brewer, P.G. (1985): Rare earth elements in the Pacific and Atlantic Oceans. *Geochim. Cosmochim. Acta* **49**, 1943-1959.

DePaulo, D.J. & Ingram, B.L. (1985): High-resolution stratigraphy with strontium isotopes. *Science* **227**, 938-941.

Dymond, J. (1981): Geochemistry of Nazca plate surface sediments: An evaluation of hydrothermal, biogenic, detrital, and hydrogenous sources. *Geol. Soc. Amer. Mem.* **154**, 133-173.

———, Corliss, J.B., Heath, G.R., Field, C.W., Dasch, E.J. & Veeh, H.H. (1973): Origin of metalliferous sediments from the Pacific Ocean. *Geol. Soc. Amer. Bull.* **84**, 3355-3372.

———, ———, Cobler, R., Muratli, M., Chou, C. & Conard, R. (1980): Composition and origin of sediments recovered by deep drilling of sediment mounds, Galapagos Spreading Center. *Initial Reports Deep Sea Drilling Project* **54**, 377-385. U.S. Gov. Printing Office, Washington, D.C.

———, ——— & Stillinger, R. (1976): Chemical composition and metal accumulation rates of metalliferous sediments from Sites 319, 320 and 321. *Initial Reports Deep Sea Drilling Project* **34**, 575-588. U.S. Gov. Printing Office, Washington, D.C.

——— & Veeh, H.H. (1975): Metal accumulation rates in the southeast Pacific and the origin of metalliferous sediments. *Earth Planet. Sci. Lett.* **28**, 13-22.

Edmond, J.M., Von Damm, K.L., McDuff, R.E. & Measures, C.I. (1982): Chemistry of hot springs on the East Pacific Rise and their effluent dispersal. *Science* **297**, 197-191.

Elderfield, H., Hawkesworth, C.J., Greaves, M.J. & Calvert, S.E. (1981): Rare-earth element geochemistry of oceanic ferromanganese nodules and associated sediments. *Geochim. Cosmochim. Acta* **45**, 513-528.

——— & Greaves, M.J. (1982): The rare-earth elements in seawater. *Nature* **296**, 214-219.

Emmermann, R., Hubberten, H.-W. & Puchelt, H. (1983): Geochemistry of basalts erupted at the Galapagos Spreading Center between 85 and 87°W. *Initial Reports Deep Sea Drilling Project* **70**, 409-418. U.S. Gov. Printing Office, Washington, D.C.

Feely, R.A., Lewison, M., Massoth, G.J., Robert-Baldo, G., Lavelle, J.W., Byrne, R.H., Von Damm, K.L. & Curl H.C., Jr. (1987): Composition and dissolution of black smoker particulates from active vents on the Juan de Fuca Ridge. *J. Geophys. Res.* **92**, 11347-11363.

Fehn, U. (1986): The evolution of low-temperature convection cells near spreading centers: A mechanism for the formation of the Galapagos Mounds and similar manganese deposits. *Econ. Geol.* **81**, 1396-1407.

Field, C.W., Wetherell, D.G. & Dasch, E.J. (1981): Economic appraisal of Nazca plate metalliferous sediments. *Geol. Soc. Amer. Mem.* **154**, 315-320.

Francheteau, J., Needham, H.D., Choukroune, P., Juteau, T., Seguret, M., Ballard, R.D., Fox, P.J., Normark, W., Carranza, A., Cordoba, D., Guerrero, J., Rangin, C., Bougault, H., Cambon, P. & Hékinian, R. (1979): Massive deep-sea sulphide ore deposits discovered on the East Pacific Rise. *Nature* **207**, 523-528.

Harder, H. (1976): Nontronite synthesis at low temperatures. *Chem. Geol.* **18**, 169-180.

Hart, S.R. (1976): LIL-element geochemistry, Leg 34 basalts. *Initial Reports Deep Sea Drilling Project* **34**, 283-288. U.S. Gov. Printing Office, Washington, D.C.

Haskin, M.A. & Haskin, L.A. (1966): Rare earths in European shales: A redetermination. *Science* **154**, 507-509.

Hays, J.D., Cook, H.E., Jenkins, G., Cook, F.M., Fuller, J.T., Goll, R.M., Milow, D. & Orr, W.N. (1972): *Initial Reports Deep Sea Drilling Project* **9**. U.S. Gov. Printing Office, Washington, D.C.

Heath, G.R. & Dymond, J. (1977): Genesis and transformation of metalliferous sediments from the East Pacific Rise, Bauer Deep, and Central Basin, northwest Nazca plate. *Geol. Soc. Amer. Bull.* **88**, 723-733.

——— & ——— (1981): Metalliferous-sediment deposition in time and space: East Pacific Rise and Bauer Basin, northern Nazca plate. *Geol. Soc. Amer. Mem.* **154**, 175-197.

Hein, J.R., Yeh, H.-W. & Alexander, E. (1979): Origin of iron-rich montmorillonite from the manganese nodule belt of the north equatorial Pacific. *Clays Clay Minerals* **27**, 185-194.

Hékinian, R., Rosendahl, B.R., Cronan, D.S., Dmitriev, Y., Fodor, R.V., Goll, R.M., Hoffert, M., Humphris, S.E., Mattey, D.P., Natland, J., Peterson, W., Roggenthen, W., Schrader, E., Scrivastava, R.K. & Warren, N. (1978): Hydrothermal deposits and associated basement rocks from the Galapagos Spreading Center. *Oceanol. Acta* **1**, 473-482.

———, ——— & Natlund, J.H. (1980): Ocean crust geothermal processes: A perspective from the vantage of Leg 54 drilling. *Initial Reports Deep Sea Drilling Project* **54**, 395-422. U.S. Gov. Printing Office, Washington, D.C.

Honnorez, J., Von Herzen, R.P., Barrett, T., Becker, K., Borella, P., Hubberten, H.-W., Jones, S., Karato, S., Laverne, C., Levi, S., Migdisov, A.A., Moorby, S.A. & Schrader, E. (1981): Hydrothermal mounds and young oceanic crust of the Galapagos: Preliminary Deep Sea Drilling results, Leg 70. *Geol. Soc. Amer. Bull.* **92**, 457-472.

———, Karpoff, A.-M. & Trauth-Badaut, D. (1983a): Sedimentology, mineralogy and geochemistry of green clay samples from the Galapagos hydrothermal mounds, Holes 506, 506C, and 507D, Deep Sea Drilling Project Leg 70 (preliminary data). *Initial Reports Deep Sea Drilling Project* **70**, 211-224. U.S. Gov. Printing Office, Washington, D.C.

———, ———, et al. (1983b): *Initial Reports Deep Sea Drilling Project* **70**. U.S. Gov. Printing Office, Washington, D.C.

Jarvis, I. (1985): Geochemistry and origin of Eocene-Oligocene metalliferous sediments from the central equatorial Pacific: Deep Sea Drilling Project sites

573 and 574. *Initial Reports Deep Sea Drilling Project* **85**, 781-804. U.S. Gov. Printing Office, Washington, D.C.

______ & Jarvis, K.E. (1985): Rare-earth element geochemistry of standard sediments: A study utilising inductively coupled plasma spectrometry. *Chem. Geol.* **53**, 335-344.

Jarvis, K.E. & Jarvis, I. (1988): Determination of the rare-earth elements and yttrium in 37 international silicate reference materials by inductively coupled plasma–atomic emission spectrometry. *Geostandards Newsletter* **12**, 1-12.

Klinkhammer, G. & Bender, M.L. (1980): The distribution of Mn in the Pacific Ocean. *Earth Planet. Sci. Lett.* **46**, 361-384.

______, Elderfield, H. & Hudson, A. (1983): Rare earth elements in seawater near hydrothermal vents. *Nature* **305**, 185-188.

______ & Hudson, A. (1986): Dispersal patterns for hydrothermal plumes in the South Pacific using manganese as a tracer. *Earth Planet. Sci. Lett.* **79**, 241-249.

Lalou, C., Brichet, E., Leclaire, H. & Duplessy, J.-C. (1983): Uranium series disequilibrium and isotope stratigraphy in hydrothermal mound samples from DSDP Sites 506-509, Leg 70, and Site 424, Leg 54: An attempt at chronology. *Initial Reports Deep Sea Drilling Project* **70**, 303-314. U.S. Gov. Printing Office, Washington, D.C.

Lawrence, J.R. & Gieskes, J.M. (1981): Constraints on water transport and alteration in the oceanic crust from the isotopic composition of pore water. *J. Geophys. Res.* **86**. 7924-7934.

Leinen, M. (1981): Metal-rich basal sediments from northeastern Pacific Deep Sea Drilling Project sites. *Initial Reports Deep Sea Drilling Project* **63**, 667-676. U.S. Gov. Printing Office, Washington, D.C.

______ (1986): Mineralogy of hydrothermal precipitates within and near active vents on the Juan de Fuca Ridge and Explorer Ridge. *EOS, Trans. Amer. Geophys. Union* **66**, 928.

______, Rea, D.K., et al. (1986): *Initial Reports Deep Sea Drilling Project* **92**. U.S. Gov. Printing Office, Washington, D.C.

Lonsdale, P. (1977): Deep-tow observations at the Mounds abyssal hydrothermal field, Galapagos Rift. *Earth Planet. Sci. Lett.* **36**, 92-110.

Lupton, J.E. & Craig, H. (1981): A major ^{3}He source at 15°S on the East Pacific Rise. *Science* **214**, 13-18.

Lyle, M. (1981): Formation and growth of ferromanganese oxides on the Nazca plate. *Geol. Soc. Amer. Mem.* **154**, 269-293.

______ (1986): Major element composition of Leg 92 sediments. *Initial Reports Deep Sea Drilling Project* **92**, 355-370. U.S. Gov. Printing Office, Washington, D.C.

______, Owen, R.M. & Leinen, M. (1986): History of hydrothermal sedimentation at the east Pacific Rise, 19°S. *Initial Reports Deep Sea Drilling Project* **92**, 585-596. U.S. Gov. Printing Office, Washington, D.C.

Marchig, V. & Gundlach, H. (1982): Iron-rich metalliferous sediments on the East Pacific Rises – prototype of undifferentiated metalliferous sediments in divergent plate boundaries. *Earth Planet. Sci. Lett.* **58**, 361-382.

______ & Erzinger, J. (1986): Chemical composition of Pacific sediments near 20°S: Changes with increasing distance from the East Pacific Rise. *Initial Reports Deep Sea Drilling Project* **92**, 371-381. U.S. Gov. Printing Office, Washington, D.C.

______, ______ & Heinze, P.-M. (1986): Sediment in the black smoker area of the East Pacific Rise (18.5°S). *Earth Planet. Sci. Lett.* **79**, 93-106.

Maris, C.R.P., Bender, M.L., Froelich, P.N., Barnes, R. & Luedtke, N.A. (1984): Chemical evidence for the advection of hydrothermal solutions in the sediments of the Galapagos Mounds hydrothermal field. *Geochim. Cosmochim. Acta* **48**, 2331-2346.

Mayer, L., Theyer, F., et al. (1985): *Initial Reports Deep Sea Drilling Project* **85**. U.S. Gov. Printing Office, Washington, D.C.

McMurtry, G.M., Veeh, H.H. & Moser, C. (1981): Sediment accumulation rate patterns on the northwest Nazca plate. *Geol. Soc. Amer. Mem.* **154**, 211-249.

______, Wang, C.-H. & Yeh, H.-W. (1983): Chemical and isotopic investigations into the origin of clay minerals from the Galapagos hydrothermal mounds field. *Geochim. Cosmochim. Acta* **47**, 475-489.

Michard, A., Albarède, F., Michard, G., Minster, J.F. & Charlou, J.L. (1983): Rare-earth elements and uranium in high-temperature solutions from East Pacific Rise hydrothermal vent field (13°N). *Nature* **303**, 795-797.

Migdisov, A.A., Gradusov, B.P., Bredanova, N.V., Bezrogova, E.V., Saveliev, B.V. & Smirnova, O.N. (1983): Major and minor elements in hydrothermal and pelagic sediments of the Galapagos Mounds Area, Leg 70, Deep Sea Drilling Project. *Initial Reports Deep Sea Drilling Project* **70**, 277-295. U.S. Gov. Printing Office, Washington, D.C.

Moorby, S.A. (1983): The geochemistry of transitional sediments recovered from the Galapagos Hydrothermal Mounds Field during DSDP Leg 70 – implications for mounds formation. *Earth Planet. Sci. Lett.* **62**, 367-376.

Natland, J.H., Rosendahl, B., Hékinian, R., Dmitriev, Y., Fodor, R.V., Goll, R.M., Hoffert, M., Humphris, S.E., Mattey, D.P., Petersen, N., Roggenthen, W., Schrader, E.L., Srivastava, R.K. & Warren, N. (1979): Galapagos hydrothermal mounds: stratigraphy and chemistry revealed by deep-sea drilling. *Nature* **204**, 613-616.

Oakman, M.R. & Leinen, M. (1985): Preliminary study of oxidized sulfide deposits from the Endeavour segment, Juan de Fuca Ridge, and Explorer Ridge. *EOS, Trans. Amer. Geophys. Union* **66**, 927.

O'Nions, R.K., Carter, S.R., Cohen, R.S., Evensen, N.M. & Hamilton, P.J. (1978): Pb, Nd and Sr isotopes in oceanic ferromanganese deposits and ocean floor basalts. *Nature* **273**, 435-438.

Oudin, E. & Cocherie, A. (1988): Fish debris record the hydrothermal activity in the Atlantis II Deep (Red Sea). *Geochim. Cosmochim. Acta* **52**, 177-184.

Piper, D.Z. (1973): Origin of metalliferous sediments from the East Pacific Rise. *Earth Planet. Sci. Lett.* **19**, 75-82.

——— & Graef, P.A. (1974): Gold and rare-earth elements in sediments from the East Pacific Rise. *Mar. Geol.* **17**, 287-297.

Rea, D.K. & Leinen, M. (1986): Neogene controls on hydrothermal activity and paleoceanography of the southeast Pacific ocean. *Initial Reports Deep Sea Drilling Project* **92**, 597-617. U.S. Gov. Printing Office, Washington, D.C.

Reynolds, P.H. & Dasch, E.J. (1971): Lead isotopes in marine Mn modules and the ore-lead growth curve. *J. Geophys. Res.* **76**, 5124-5129.

Robertson, A.H.F. (1976): Origin of ochres and umbers: evidence from Skouriatissa, Troodos Massif, Cyprus. *Trans. Inst. Mining Metall.* **B85**, 245-252.

Rona, P.A. (1980): TAG Hydrothermal Field: Mid-Atlantic Ridge crest at latitude 26°N. *J. Geol. Soc. Lond.* **137**, 385-402.

Ruhlin, D.E. & Owen, R.M. (1986): The rare earth element geochemistry of hydrothermal sediments from the East Pacific Rise: Examination of a seawater scavenging mechanism. *Geochim. Cosmochim. Acta* **50**, 393-400.

Sayles, F.L. & Bischoff, J.L. (1973): Ferromanganese sediments in the equatorial east Pacific. *Earth Planet. Sci. Lett.* **19**, 330-336.

———, Ku, T.L. & Bowker, P.C. (1975): Chemistry of ferromanganese sediment of the Bauer Deep. *Geol. Soc. Amer. Bull.* **86**, 1423-1431.

Scott, M.R., Scott, R.B., Rona, P.A., Butler, L.W. & Nalwalk, A.J. (1974): Rapidly accumulating manganese deposit from the median valley of the Mid-Atlantic Ridge. *Geophys. Res. Lett.* **1**, 355-358.

Scott, S.D., Barrett, T.J., Hannington, M., Chase, R.L., Fouquet, Y. & Juniper, K. (1984): Tectonic framework and sulfide deposits of Southern Explorer Ridge, northeastern Pacific Ocean. *EOS, Trans. Amer. Geophys. Union* **65**, 1110.

Shearme, S., Cronan, D.S. & Rona, P. (1983): Geochemistry of sediments from the TAG geothermal field, Mid-Atlantic Ridge at 26°N. *Mar. Geol.* **51**, 269-291.

Stacey, J.S. & Kramers, J.D. (1975): Approximation of terrestrial lead isotopes evolution by a two-stage model. *Earth Planet. Sci. Lett.* **26**, 207-221.

Sun, S.-S. (1980): Lead isotopic study of young volcanic rocks from mid-ocean ridges, ocean islands and islands arcs. *Philos. Trans. Roy. Soc. London* **297A**, 409.

Tatsumoto, M. (1978): Isotopic composition of lead in oceanic basalt and its implication to mantle evolution. *Earth Planet. Sci. Lett.* **38**, 63-87.

Thomson, J., Carpenter, M.S.N., Colley, S., Wilson, T.R.S., Elderfield, H. & Kennedy, H. (1984): Metal accumulation rates in northwest Atlantic pelagic sediments. *Geochim. Cosmochim. Acta* **48**, 1935-1948.

Tracey, J.I., Sutton, G.H., et al. (1971): *Initial Reports Deep Sea Drilling Project* **8**. U.S. Gov. Printing Office, Washington, D.C.

Turner, D.R., Whitfield, M. & Dickson, A.G. (1981): The equilibrium speciation of dissolved components in freshwater and seawater at 25°C and 1 atm pressure. *Geochim. Cosmochim. Acta* **45**, 855-881.

Unruh, D.M. & Tatsumoto, M. (1976): Lead isotopic composition and uranium, thorium and lead concentrations in sediments and basalts from the Nazca Plate. *Initial Reports Deep Sea Drilling Project* **34**, 341-347. U.S. Gov. Printing Office, Washington, D.C.

Van Andel, T.H., Heath, G.R., et al. (1973): *Initial Reports Deep Sea Drilling Project* **16**. U.S. Gov. Printing Office, Washington, D.C.

Varnavas, S.P., Moorby, S.A. & Cronan, D.S. (1983): Partition geochemistry of sediments from holes 506 and 509B, DSDP Leg 70. *Initial Reports Deep Sea Drilling Project* **70**, 297-302. U.S. Gov. Printing Office, Washington, D.C.

Varenstsov, I.M., Sakharov, B.A., Drits, V.A., Tsipursky, S.I., Choporov, D.Y. & Aleksandrova, V.A. (1983): Hydrothermal deposits of the Galapagos Rift zone, Leg 70: Mineralogy and geochemistry of major components. *Initial Reports Deep Sea Drilling Project* **70**, 235-268. U.S. Gov. Printing Office, Washington, D.C.

Veizer, J. & Compston, W. (1974): ^{87}Sr/^{86}Sr composition of seawater during the Phanerozoic. *Geochim. Cosmochim. Acta* **38**, 1461-1484.

Vidal, Ph. & Clauer, N. (1981): Pb and Sr isotopic systematics of some basalts and sulfides from the East Pacific Rise at 21°N (project RITA). *Earth Planet. Sci. Lett.* **55**, 237-246.

Von Damm, K.L., Edmond, J.M., Grant, B. & Measures, C.I. (1985): Chemistry of submarine hydrothermal solutions at 21°N, East Pacific Rise. *Geochim. Cosmochim. Acta* **49**, 2197-2220.

von der Borch, C.C., Nesteroff, W.D. & Galehouse, J. (1971): Iron-rich sediments cored during Leg 8 of the Deep Sea Drilling Project. *Initial Reports Deep Sea Drilling Project* **8**, 829-835. U.S. Gov. Printing Office, Washington, D.C.

Weiss, R.F., Lonsdale, P., Lupton, J.E., Bainbridge, A.E. & Craig, H. (1977): Hydrothermal plumes in the Galapagos Rift. *Nature* **267**, 600-603.

White, W.M. (1979): Pb isotope geochemistry of the Galapagos Islands. *Carnegie Inst. Washington Year Book* **78**, 331-335.

Williams, D.L., Green, K.E., Van Andel, T.H., Von Herzen, R.P., Dymond, J.R. & Crane, K. (1979): The hydrothermal mounds of the Galapagos rift: Observations with DSRV Alvin and detailed heat flow studies. *J. Geophys. Res.* **84**, 7467-7484.

Yeats, R.S., Hart, S.R. et al. (1976): *Initial Reports Deep Sea Drilling Project* **34**. U.S. Gov. Printing Office, Washington, D.C.

Yeh, H.-W. & Savin, S.M. (1977): Mechanism of burial metamorphism of argillaceous sediments: 3. O-isotope evidence. *Bull. Geol. Soc. Amer.* **88**, 1321-1330.

Zindler, A., Jagoutz, E. & Goldstein, S. (1982): Nd, Sr and Pb isotopic systematics in a three-component mantle: a new perspective. *Nature* **298**, 519-523.

Received June 3, 1987; revised manuscript accepted July 12, 1988.